

**Constitutive AP-1 Activity and EBV Infection Induce PD-L1 in Hodgkin
Lymphomas and Post-transplant Lymphoproliferative Disorders:
Implications for Targeted Therapy**

Running title: AP-1 Activity and EBV Infection Induce PD-L1

Michael R. Green^{1,2,□}, Scott Rodig³, Przemyslaw Juszczynski^{1,2,□}, Papiya Sinha³, Jing
Ouyang^{1,2} Evan O'Donnell¹, Donna Neuberg¹, Margaret A. Shipp^{1,2,*}

¹ Dana-Farber Cancer Institute, Boston, MA 02115;

² Harvard Medical School, Boston, MA 02115;

³ Brigham and Womens Hospital, Boston, MA 02115;

□ Current address: Stanford University, Stanford, CA;

□ Current address: Institute of Hematology and Transfusion Medicine, Warsaw, Poland

*Corresponding author: Margaret A. Shipp, Dana-Farber Cancer Institute, 450 Brookline

Avenue, Boston, MA 02215; Phone: 617-632-3874; Fax: 617-632-4734; Email:

margaret_shipp@dfci.harvard.edu

Supplemental Figure Legends

Figure S1: PD-L1 transcript abundance in normal B-cells, primary cHLs and DLBCLs. PD-L1 transcript abundance was assessed using publicly available gene expression profiles (1) (GEO accession, GSE12453). Raw cel files were normalized by Robust Multiarray Preprocessing using the default setting of ArrayExpress software, and visualized using dChip software. A) Relative differences in PD-L1 expression (probes 205841_at and 20582_at) in normal B cells (naïve, centroblasts [C.blast], centrocytes [C.cyte], memory cells and plasma cells [P. cells]), DLBCLs and cHLs. The pinkogram was generated with the D-Chip program. Color scale at the bottom indicates relative expression +/- SEM. Red connotes high-level expression; blue indicates low-level expression. The cHLs have significantly more abundant PD-L1 transcripts than normal B cells ($p < .001$) and DLBCLs ($p = .025$). B) Box plots of PD-L1 probe fluorescence intensities in the respective cell types in A.

Figure S2: Comparative induction of PD-L1 compared to PD-L2 by AP-1. A) Diagrammatic representation of the PD-L2 regulatory elements including the previously described PD-L2 promoter element containing the JAK/STAT-responsive ISRE/IRF1 module (2), and a newly identified potential enhancer element containing NF κ B and cREL binding sites. In contrast to PD-L1, no predicted AP-1 binding sites were found in highly conserved regions within intron 1 of the PD-L2 gene. B) Publicly available ChIP-seq data for cJUN binding in three non-lymphoid cell lines or cell types (Hela, HuVEC, K562) over the predicted AP-1 sites in the candidate PD-L1 enhancer. ChIP-seq signals were highest over the first of the two predicted binding sites, which was deleted in PD-L1 luciferase constructs (Fig. 2A and C). C) PD-L1 promoter- and enhancer-driven luciferase activity in the L540 cHL cell line. Constructs as in Fig. 2C. Data are averages of three independent experiments. D) PD-L2 transcript abundance in cHL cell lines

following overexpression of a cJUN dominant-negative (c-JUNDN) construct. Enforced expression of a dominant-negative cJUN (cJUNDN) in HL cell lines did not alter PD-L2 transcript abundance, consistent with the absence of a predicted AP-1-responsive enhancer element in PD-L2. Data are averages of three independent experiments.

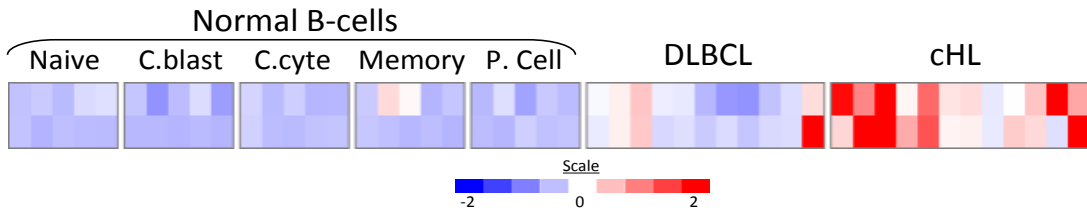
Figure S3: EBV and PD-L1 expression. A) Flow cytometric analysis of cell surface PD-L1 abundance in a panel of EBV-transformed lymphoblastoid cell lines (LCLs). Data are representative of three independent experiments. B) Heat map and bar graph showing probe intensities of a PD-L1 specific probe (223834_at) from a publicly available dataset containing transcript data for normal GCB cells and GCB cells expressing LMP1 (3) (GEO accessions, GSE10821 and GSE10831) and processed as previously described (4). Expression of LMP1 significantly increased PD-L1 probe fluorescence intensity ($p=.001$). C) CHIP-coupled PCR showing binding of the PD-L1 enhancer region by both cJUN and JUN-B in the EBV-transformed LCL, NOR. Binding was lower than that observed in HL cell lines, but PCR amplification of DNA immunoprecipitated with cJUN and JUN-B antibodies yielded markedly stronger bands than that from the control antibody. Data are representative of two independent experiments. D) Intracellular phosphoflow cytometric analyses of phosphorylated STAT1, STAT3, STAT5 and STAT6 in the panel of EBV-transformed LCLs. The EBV-transformed LCLs have only low levels of pSTAT1 and pSTAT6, but have higher levels of the JAK3-associated STATs, pSTAT3 and pSTAT5. Data are representative of three independent experiments.

References

1. Brune V, Tiacci E, Pfeil I, Doring C, Eckerle S, van Noesel C, et al. Origin and pathogenesis of nodular lymphocyte - predominant Hodgkin lymphoma as revealed by global gene expression analysis. *J Exp Med* 2008; 205: 2251-68.
2. Green MR, Monti S, Rodig SJ, Juszczynski P, Currie T, O'Donnell E, Chapuy B, Takeyama K, et al. Integrative analysis reveals selective 9p24.1 amplification, increased PD-1 ligand expression, and further induction via JAK2 in nodular sclerosing Hodgkin lymphoma and primary mediastinal large B-cell lymphoma. *Blood* 2010; 116: 3268-77; PMID: PMC2995356.
3. Vockerodt M, Morgan S, Kuo M, Wei W, Chukwuma M, Arrand J, et al. The Epstein-Barr virus oncoprotein, latent membrane protein-1 reprograms germinal centre B cells towards a Hodgkin's Reed-Sternberg-like phenotype. *J Pathol* 2008; 216: 83-92.
4. Ouyang J, Juszczynski P, Rodig SJ, Green MR, O'Donnell E, Currie T, et al. Viral induction and targeted inhibition of galectin-1 in EBV+ post-transplant lymphoproliferative disorders. *Blood* 2011; 117: 4315-22; accompanying editorial, *Blood* 2011; 117:4165-6, cited in *SciBx* 4(9); doi:10.1038/scibx2011251 2011.

Figure S1

A.



B.

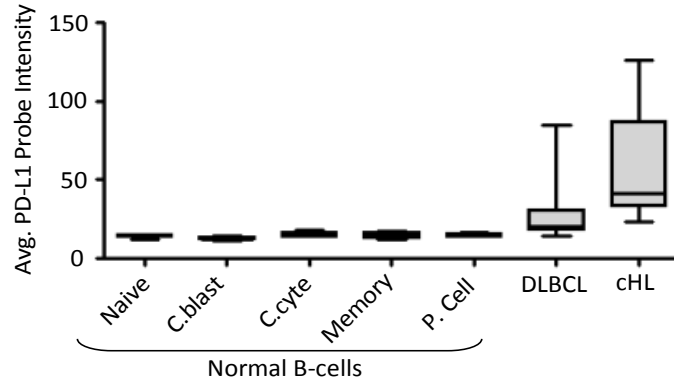


Figure S2

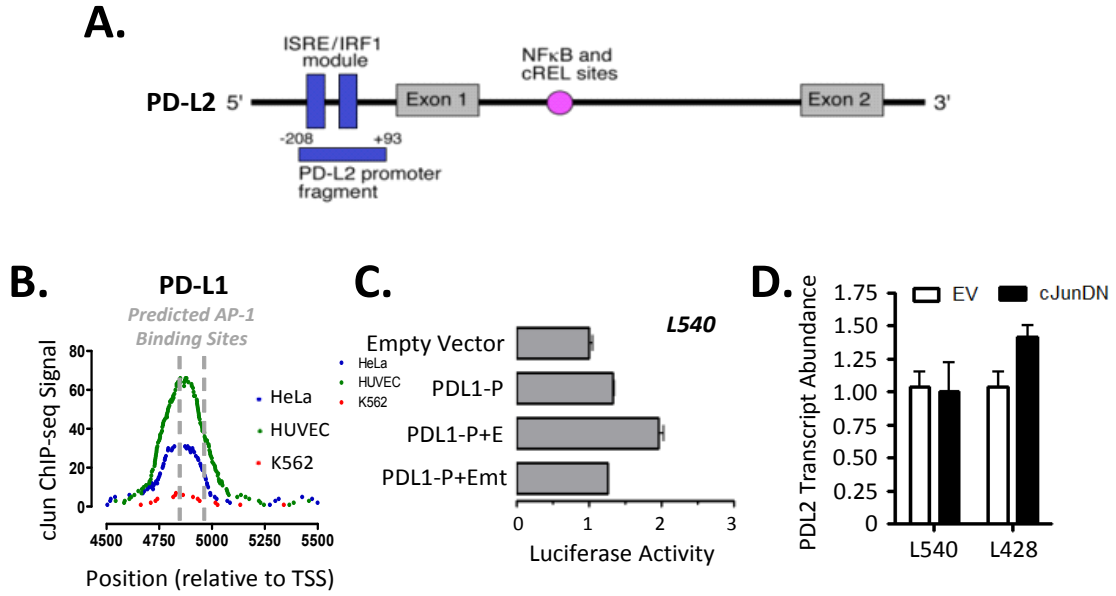


Figure S3

